Reason - A Technical Journal
ISSN 2277–1654
Volume - XV ● 2016

SIMULATION OF SUPERCRITICAL BEND FLOW THROUGH AN OPEN CHANNEL

Rupak Saha[1], Sanchayan Mukherjee[2], Ajay Kumar Das[3], Kanhu Keshab Jena[4], Manajit Mandal[5] and Pranab Kumar Gorh[6]

Department of Mechanical Engineering, Kalyani Government Engineering College,
Kalyani- 741235, Nadia, West Bengal, India
Email: [1]saharupak4@gmail.com, [2]sanchayan02@yahoo.com, [3]ajaydas280@gmail.com
[4]kanhukeshabjena@gmail.com, [5]manajit2014&@gmail.com, [6]kpranab52@gmail.com.

Paper received on: June 06, 2016, accepted after revision on: July 14, 2017
DOI:10.21843/reas/2016/22-31/158773

Abstract: The present work investigates turbulent supercritical (Froude Number>1) bend flow through an open channel. The CFD-based model, ANSYS FLUENT version 13.0, is used to solve the three-dimensional (3D) continuity and Navier-Stokes equations. The standard $k = \varepsilon$ turbulence model is considered for the investigation. The model is applied to the channel bend geometry as described in a published experimental work. Results in the form of velocity profiles and non-dimensional water depths are obtained and compared with the already published experimental findings. The results obtained through the present work as compared to the published ones indicate that three-dimensional modelling technique plays a significant role in the entire endeavour and, thus, the three-dimensional approach makes highly-improved predictions. Also, the three-dimensional simulation indicates the existence of a nonlinear gradient of water depth as the water flows through the bend.

Keywords: Supercritical Flow; Froude Number; Channel Bend; Turbulence.

Notations

b = channel width (m)
F = Froude number (–)
h = water depth (m)
h_0= approach water depth (m)
S= bottom slope (%)
k = turbulent kinetic energy ($m^2 s^{-2}$)
p = pressure (Pa)
Q = discharge rate ($m^3 s^{-1}$)
R = axial curvature radius (m)
t = time (s)
u_i= velocity components ($m s^{-1}$)
t = time (s)
α = volume fraction (–)
β = deflection angle (°)
ε = turbulent dissipation rate ($m^2 s^{-3}$)
μ = dynamic viscosity ($kg m^{-1} s^{-1}$)
μ_t = eddy viscosity ($kg m^{-1} s^{-1}$)
ν = kinematic viscosity ($m^2 s^{-1}$)
θ= angular coordinate (°)
ρ = fluid density ($kg m^{-3}$)

1. INTRODUCTION

Channels of non-linear alignment under supercritical conditions are quite common in hydraulic structures, e.g., spillways, chutes, as well as sewer systems. These irregular boundaries cause the supercritical flow to choke and generate shock-waves. In the case of a supercritical bend flow, apart from the super elevation that represents the action of centrifugal force on the flow, these shock-waves cause an excessive rise in the free surface, causing further complications. Thus, the provision required for sidewall heights, to prevent overtopping, is of particular importance. The outer wall that is curved towards the centre of the bend, obstructs and retards the flow and, consequently, the flow depth increases. On the other hand, the inner wall that curves outwardly accelerates the flow and causes a decrease in the flow depth. Thus, the advent of the curvature at the opposite walls acts as the origin of flow disturbances, with two disturbance lines crossing the stream and successively reaching the opposite sides. This results in disturbances in the form of two cross-waves starting on opposite sides and reflecting back and forth between the walls.

Of late, considerable effort has been made to investigate supercritical bend flow. These works may broadly be classified into: (1) analytical study, (2) experimental investigation, and (3) numerical modelling. Poggi [1] investigated the supercritical bend flow through experiments. Tahershamsi [2] experimentally investigated the behaviour of supercritical flows in bends with circular cross-sections. Dammuller et al. [3] dealt with transient supercritical flows in channel bends numerically, using a two dimensional model. Reinauer and Hager [4] studied the phenomenon of supercritical flow in smooth horizontal bends both analytically and experimentally. They conducted experiments in three bends with relative curvatures of 0.07, 0.144, and 0.31 with deviation angles equal to 51°, 51° and 30° both, and 30°, respectively. Later on, Frazão and Zech [5] analyzed a dam-break flow in an initially dry channel with a 90°-bend both numerically and experimentally. Beltrami et al. [6] did experiments to judge the suitability of a novel approach of regularizing supercritical flow profiles in channel bends. They placed water flaps at the inner wall, upstream of a 180°-curve, to induce a counter-phase disturbance pattern. They arrived at a conclusion that the water flaps, by causing a reduction from 30% to 80% of the wave amplitude, modulate the flow pattern significantly.

The present work consists of computer-aided analysis of a supercritical bend flow through an open channel. The results obtained are compared to those obtained experimentally by Poggie [1].

2. METHODOLOGY

2.1. Governing Equations

The two principles that govern the physical nature of all fluid flows are the conservation of mass and of momentum. The mathematical representation of these two principles is known as the continuity and Navier-Stokes equations, respectively, for which a 3D unsteady Newtonian flow field with a constant density in a Cartesian coordinate system are as follows:

Continuity equation:

Navier-stokes equation:

$$\frac{\partial u_i}{\partial x_i} = 0 \tag{1}$$

$$\partial u_i / \partial t + u_j \partial u_i / \partial x_j = -(1/\rho)(\partial p / \partial x_i) + \nu(\partial^2 u_i / \partial x_j^2) + X_i \tag{2}$$

Where variable u_i represents the velocity component in the Cartesian coordinate system, t is the time, p is the pressure, ρ is the fluid density, ν is the kinematic viscosity, and the X_i term refers to the body force per unit mass. Most of the time, the gravity force is the only body force. The terms on the left hand-side of the Navier-stokes equations indicate the total accelerations which are the sum of the local acceleration caused by an unsteady motion and the convective accelerations resulting from changes in velocity over position. The right hand side indicates the pressure and shear stresses.

If the Reynolds stresses are to be included in the problem, a turbulence model will be needed for the closure of the system of mean flow equations. Here, the two equation standard *k*-*ε* model [7], based on the Boussinesq hypothesis, is employed for its wide applications in engineering purposes.

The equations of the standard *k*-*ε* model consist of:

$$\nu_t = C_\mu \frac{k^2}{\varepsilon} \tag{3}$$

$$\frac{\partial k}{\partial t} + \frac{\partial \overline{u}_i k}{\partial x_j} = \frac{\partial}{\partial x_j}\left(\frac{\nu_t}{\sigma_t}\frac{\partial k}{\partial x_j}\right) + p - \varepsilon \tag{4}$$

$$\frac{\partial \varepsilon}{\partial t} + \frac{\partial \overline{u}_i \varepsilon}{\partial x_j} = \frac{\partial}{\partial x_j}\left(\frac{\nu_t}{\sigma_\varepsilon}\frac{\partial \varepsilon}{\partial x_j}\right) + C_{1\varepsilon}\frac{\varepsilon}{k} p - C_{2\varepsilon}\frac{\varepsilon^2}{k} \tag{5}$$

Where ν_t is the eddy kinematic viscosity and is calculated in terms of the turbulent kinetic energy, *k*, and the turbulent dissipation rate, *ε*. Table 1 presents the values of empirical constants as suggested by Masoud et al. [7].

Table 1: Values of Empirical Constants

C_μ	$C_{1\varepsilon}$	$C_{2\varepsilon}$	σ_k	σ_ε
0.09	1.44	1.92	1.00	1.33

2.2. Numerical Approach

2.2.1. Mesh Generation

To perform numerical modelling, the geometry of flow field needs to be defined first. This is achieved with the help of SOLID WORKS 2014. The product geometry is then transferred to the ANSYS FLUENT 13.0, in which a mesh generating pre-processor is available. Once the geometry is created, the entire computational domain needs to be decomposed into non-overlapping small cells named “control volumes” through the mesh generation process. The execution time of computations from CFD modelling and the resulting accuracy and degree of consistency with the experimental results depends on the gridding size. A number of different grids of various sizes are examined in order to model this experimental study and to consider the initial results obtained. In addition, the grid is selected in such manner that it would be in line with the flow direction. As it approaches the bend the grid becomes smaller. The grid becomes larger at the exit of the bend. This is done to save computation time.

The volume of fluid method (VOF) for dealing with the large anticipated free-surface curvature is adopted for this work. The main problem of this method is the high-resolution mesh required to accurately model the free-surface. Thus, to provide a precise presentation of the present complex free-surface, the vertical grid spacing was set at 3 mm and the aspect-ratio of 5:1 was used. After 2000 iterations it attained steady state.

2.2.2. Free-Surface Modelling

In terms of open-channel hydraulics, a free-surface is defined as a boundary which is formed between two phases, liquid and gas (here, water and air). Anticipating a considerable free-surface deformation, the Volume of Fluid (VOF) method is adopted to draw the complex behaviour of the free-surface.

The VOF method holds the assumption of phases' immiscibility i.e., the VOF method does not allow the phases' interpenetration. An extra scalar, α, to define the volume fraction filled with a specific phase in each of the computational cells, appears in the VOF method formulation. According to the concept of volume fraction and defining the volume fraction of i^{th} phase in a computational cell as $\alpha_i = V_i / V_{ceu}$ and V = volume, a scalar value of one implies a cell full of the phase and correspondingly, a zero value indicates a cell empty of the phase. Then, any scalar values between zero and one will identify a partially-filled cell whose remaining volume is occupied by the second phase, thus containing the free-surface.

2.2.3. Computational Algorithms

The implicit pressure-based solver of FLUENT, with a first-order time-dependent formulation is then applied to the model equations which are discretized with the mass conserving finite-volume method. The discretization of the advective-diffusive terms in the momentum equation as well as the k and ε terms is performed using a first-order upwind scheme. For the pressure-velocity coupling, a Pressure Implicit with Splitting of Operators (PISO) algorithm, of the SIMPLE family with one additional pressure correction equation, is employed. The PISO algorithm proved successful for transient flow calculations. The PREssure Stagnation Option, or PRESTO! algorithm, which is recommended for the VOF simulations, is utilized for the pressure interpolation scheme. Such interpolation is necessary to define the pressure values at the cell faces based on those stored at the adjacent cell centres.

2.2.4. Boundary Conditions

Specifying the flow variables on the solution domain boundaries is crucial in order to accurately define the hydrodynamic behaviour of the flow. In this regard, different types of boundary conditions are provided by FLUENT among which four, namely, Mass flow inlet, Pressure-Outlet, Symmetry, and Wall, are here adopted and will be presented in the following.

At the upstream border of the computational domain, the channel's entry section is the mass flow inlet. Being an open channel flow, the mass flow inlet is a multiphase (air and water) inlet. Such geometrical separation of the water flow and airflow guarantees the accurate imposition of approach flow depth at the inlet. Considering the supercritical condition of the flow, two upstream boundary conditions are required to completely introduce the approach flow. Thus, an approach height boundary condition is applied to the water-inlet as the second necessary boundary condition. Likewise, at the channel outlet boundary a Pressure-Outlet condition with the atmospheric pressure constraint provides a free flow. A No-Slip Wall condition enforcing zero velocity components is set at the side walls of the channel as well as its bottom. At the channel top boundary, which is in contact with air, a Symmetry condition is imposed and implies that there would be zero value of the normal velocity component as well as the normal gradients of all variables.

In turbulence modelling, at the inlet and outlet boundaries, the turbulent scalar quantities, k and ε, are set as their default values, 1 and 1, respectively. Also, at the wall boundaries, the standard wall function approach is applied to model the near-wall region.

Initially, the calculation considers the channel empty and initial valuation assigns the 0 value to all flow variables, except the turbulent kinetic energy and the turbulent dissipation rate, to which the value of 1 is assigned.

3. EXPERIMENTAL SETUP

The model was applied to the channel bend of the same rectangular cross-section. The physical domain dimensions and the flow characteristics of the simulation are considered the same as the experiments of Poggi [1] for the sake of comparison between the results. Table 2 presents geometric details of the channel.

Table 2: Geometric Details of the Channel

B (°)	*R* (m)	*S* (%)	*B* (m)
45°	3	5	0.25

Here, β = Deflection angle

R = Radius of curvature (m)

S = Bottom slope (%)

b = Channel width (m)

Table 3 shows the flow details of the test case as described in [1].

Table 3: Flow Details of the Test Case

h_o (m)	F	Q (l/s)
0.0993	3.04	74.47

Here, h_0 = Approach water depth (m)

F = Froude number

Q = volume flow rate (litre/sec)

In an attempt to find the possible factors responsible for the existing gap between the experimental data and the previous numerical predictions, the effects of two factors on the results are studied, e.g., (i) the three-dimensionality, and (ii) the turbulence. The results herein presented consist of the dimensionless water surface profiles along four longitudinal sections, i.e., 1, 2, 3, and 4, which are located at 0.05, 0.1, 0.15, and 0.2 m distance from the outer wall, respectively.

As mentioned earlier, the simulation is used to examine the water surface profile and velocity distribution at the given planes in the channel. These values are finally compared with the values obtained in Poggi's experiment [1].

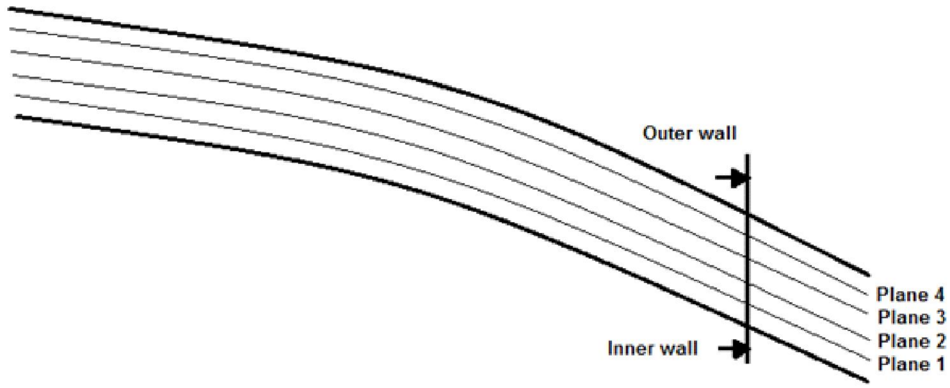

Fig.1 Location of Longitudinal sections along the channel bend

Apart from this, velocity profiles are also drawn considering four transverse planes along the channel, as shown in Fig. 2, to compare with the experimental investigations. The four planes are along transverse direction separated from each other by 0.45 m. Fig. 3 shows the angular coordinates measured from one end of the bend as envisaged in [4].

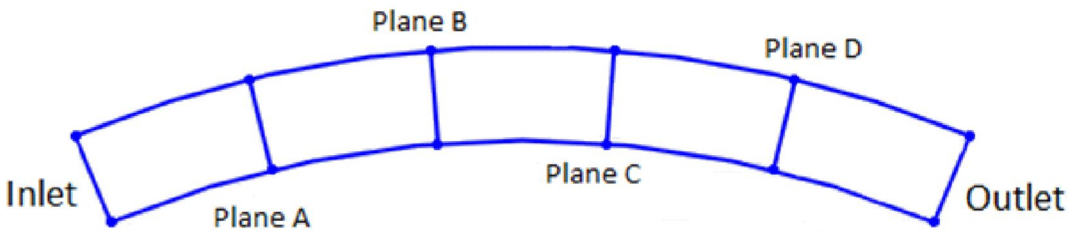

Fig. 2 Transverse Section locations along the bend channel

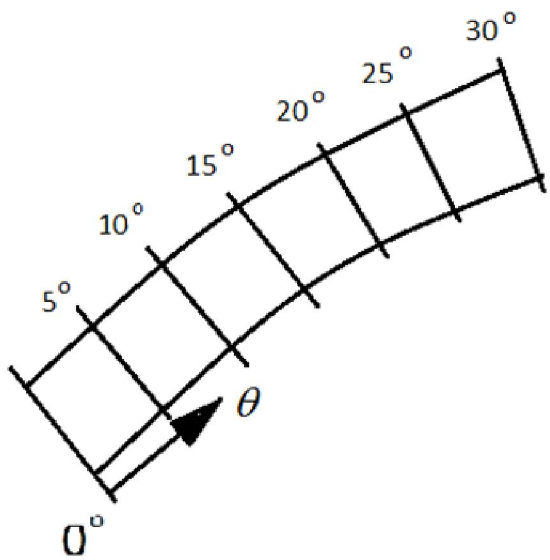

Fig. 3 Angular Coordinates (measured from one end of the bend)

4. RESULTS AND DISCUSSION

Water surface profile in the form of non-dimensional water profile is used to compare with the experimental investigation. The non-dimensional water profile is drawn along the four sections as shown in Fig. 1.

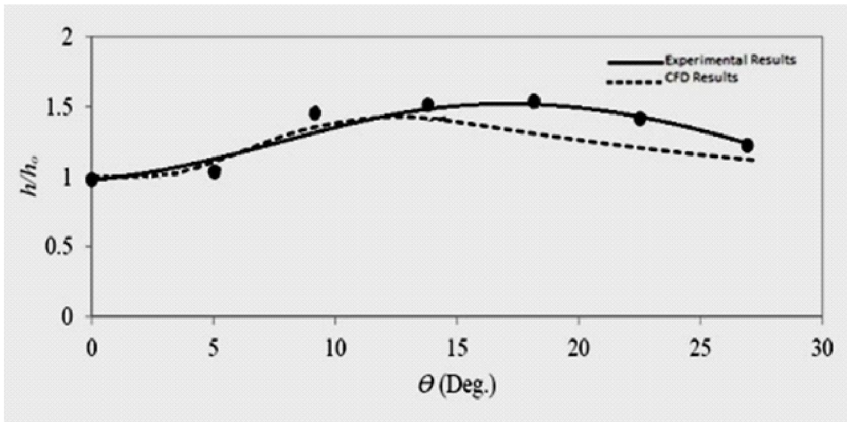

Fig. 4 Plot of non dimensional water depth with the angular coordinate along Sec. 1

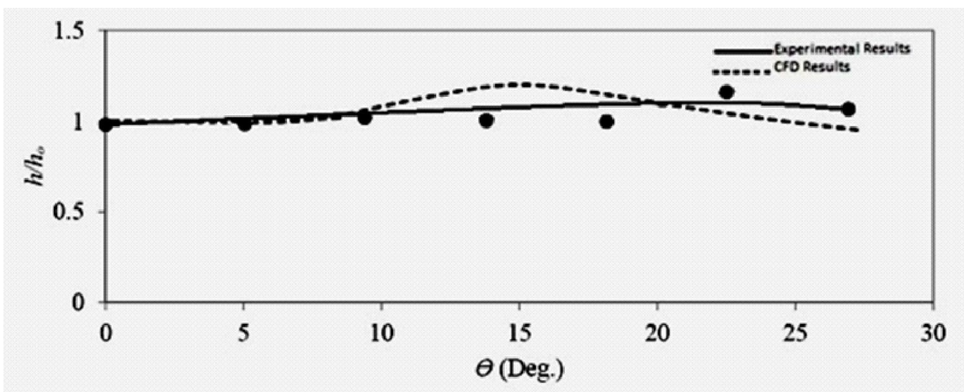

Fig. 5 Plot of non dimensional water depth with angular coordinate along Sec. 2

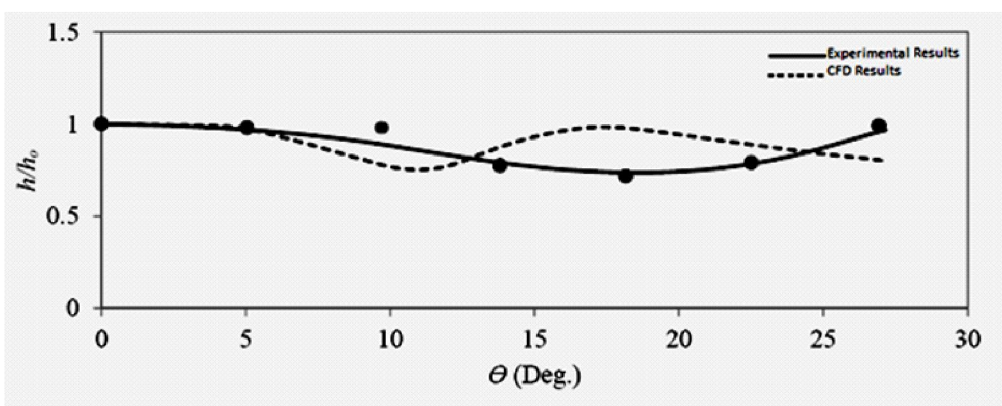

Fig. 6 Plot of non dimensional water depth with angular coordinate along Sec.3

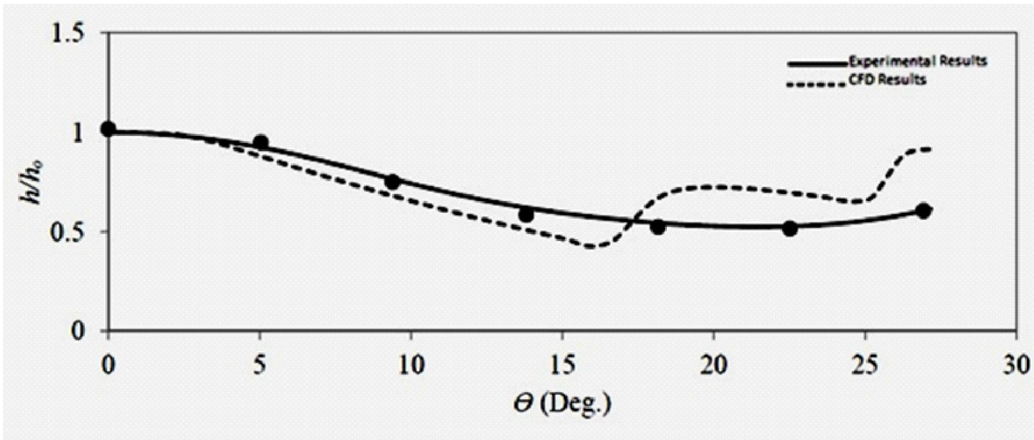

Fig. 7 Plot of non dimensional water depth with angular coordinate along Sec.4

From these results, it is evident that in supercritical bend flow there is a super elevation of the water column along the outer wall for which with the increase of angular coordinate (θ) the flow height has a positive slope along the Section 1. But the flow height has decreased along the inner wall for which there is a negative slope found in case of Section 4. So, the result indicates the presence of nonlinear transverse water slope.

Fig. 7–10 indicate the velocity profiles varying with channel width in different transverse planes as shown in Fig. 2. They show the values obtained through the present work compared with those obtained through Poggi's [1] experiments.

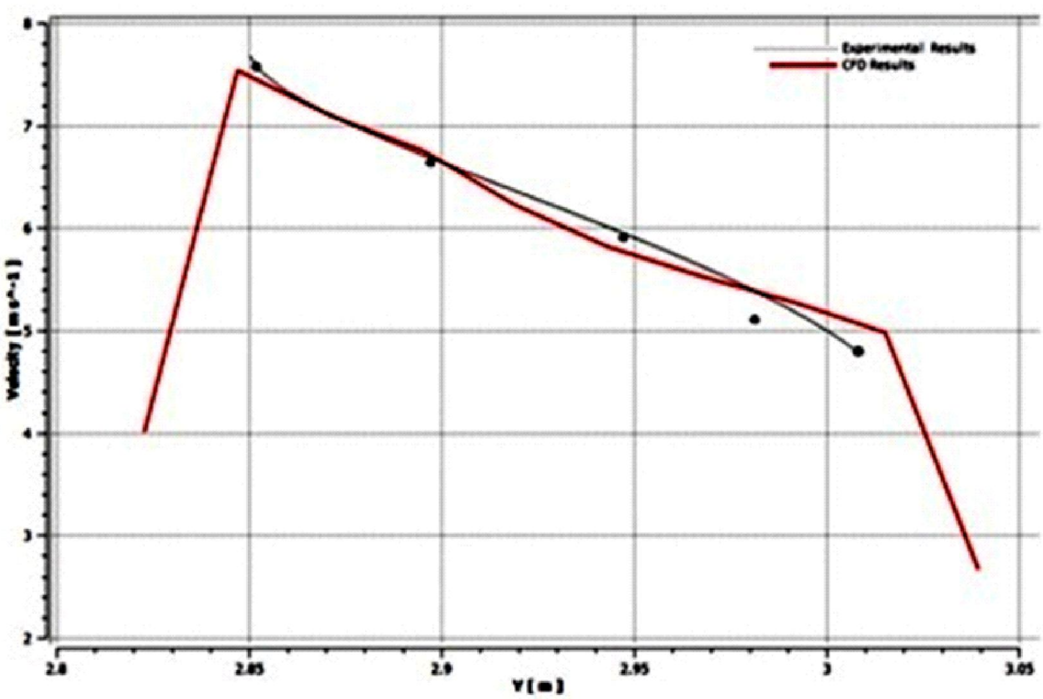

Fig. 8 Plot of velocity profile with channel width on the plane A

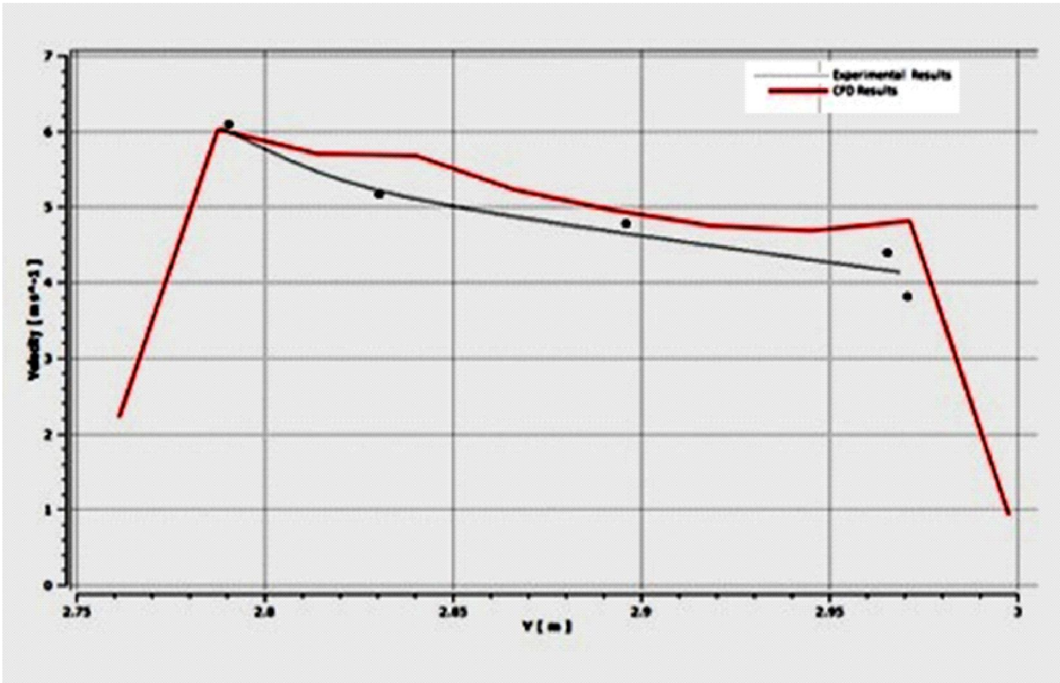

Fig. 9 Plot of velocity profile with channel width on the plane B

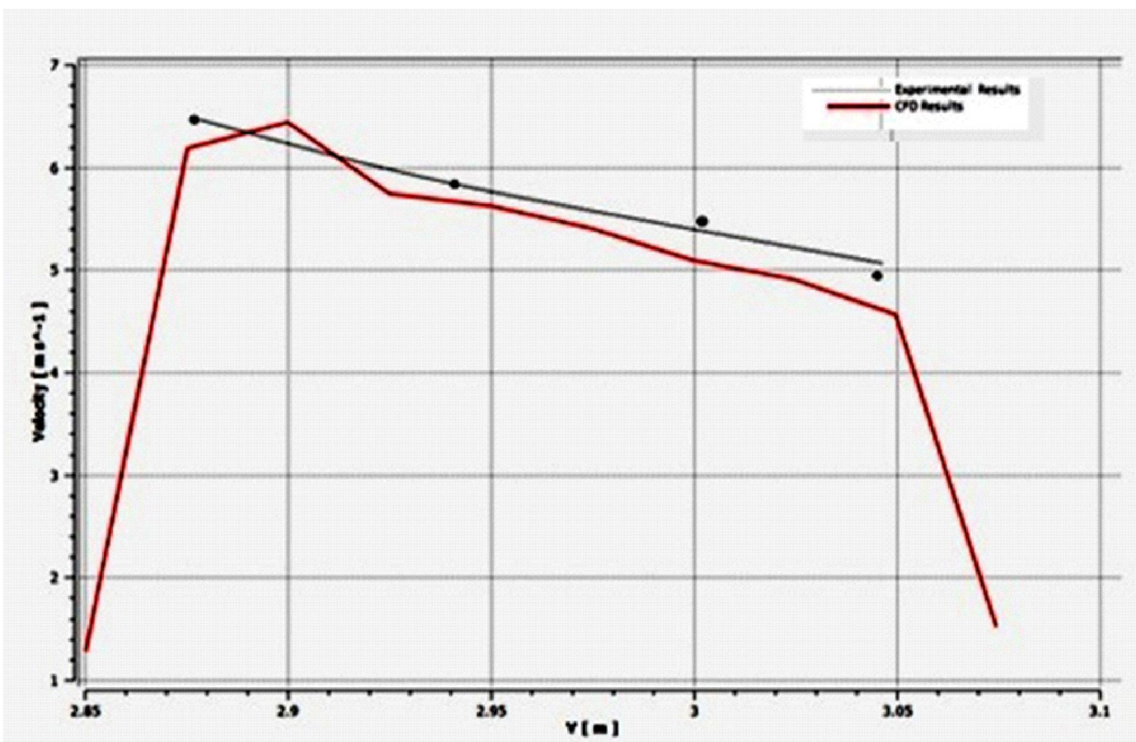

Fig. 10 Plot of velocity profile with channel width on the plane C

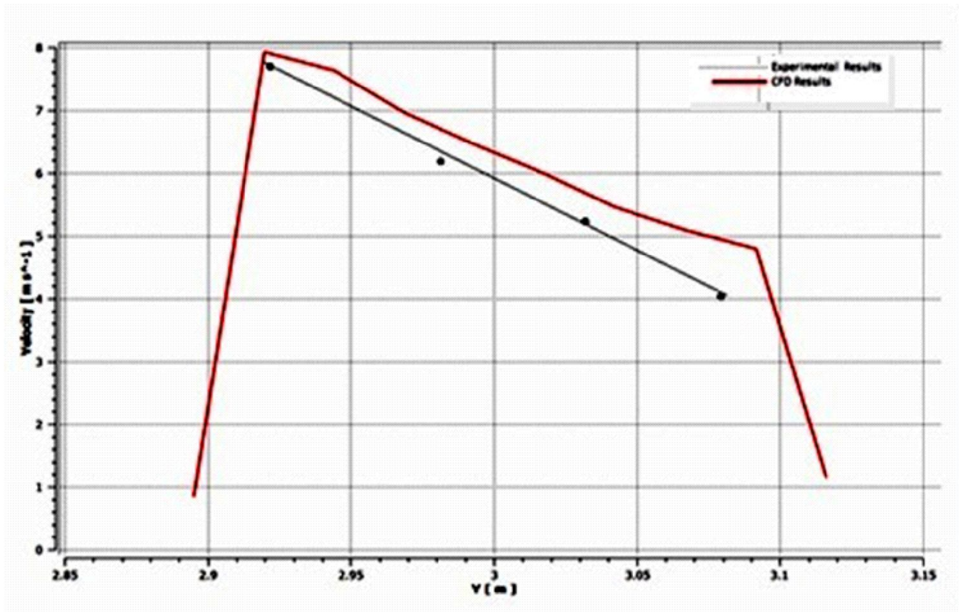

Fig. 11 Plot of velocity profile with channel width on the plane D

From this velocity profile along the transverse plane A i.e. along the width, there is acceleration taking place near the inner wall whereas there is deceleration in the vicinity of the outer wall. Similar results are obtained for all other planes.

As in the work the walls are stationary walls with no slip conditions (roughness constant=0.5), there are sudden drop in velocity near both of the walls (inner and outer).

5. Conclusion

This present work deals with simulation of the effect of supercritical bend flow through channel using the CFD model. The 3D simulation indicates the existence of a nonlinear gradient of water depth while flowing through the bend. Due to centrifugal force, this super elevation takes place. This also gives the velocity gradient along the channel width. The presence of centrifugal force results in a secondary flow along the transverse direction of the main flow. Results of the present analysis match quite well with Poggi's Experimental results. In light of the above discussion, it can be concluded that the CFD model is capable of predicting the general flow pattern quite accurately for a supercritical flow in a channel bend.

References

[1] Poggi, B, Correntive Locinei Canali in Curva (High-speed Flow in Curved Chutes). *L'Energia Elettrica*, Vol. 33, No. 7, pp. 465-480, 1956 [in Italian].

[2] Tahershamsi, A., The Effect of Bends upon Surface Waves in Open Channels of Circular Cross Section. *PhD Thesis*, Department of Civil and Structural Engineering, University of Manchester, Institute of Science and Technology UK, pp. 235-257, 1988.

[3] Dammuller, D.C., Bhallamudi M. and Chaudhry M.H., Modeling of Unsteady Flow in Curved Channels. *Hydraulic Engineering*, Vol. 115, No. 11, pp. 1479-1494, 1989.

[4] Reinaure, R. and Hager W.H. Supercritical Bend Flow. *Hydraulic Engineering*, Vol. 123, No. 3, pp. 208-218, 1997.

[5] Frazão S.S. and Zech Y. Dam-Break in Channels with 90° Bend. *Hydraulic*

Engineering, Vol. 128, No. 11, pp. 956-968, 2002.

[6] Beltrami, G.M., Repetto R. and Guzzo A.D., A Simple Method to Regularize Supercritical Flow Profiles in Bends. *Hydraulic Research*, Vol. 45, pp. 773-786, 2007.

[7] Masoud, M.N., Reyhaneh-Sadat, G.H. and Mahnaz, G.H., 3-D Numerical Simulation of Supercritical Flow in Bends of Channel, *Proceedings of International Conference on Mechanical, Automotive and Materials Engineering*, Dubal, pp. 167-171, Jan 7-8, 2012.